

GEODETIC SURFACE BASED METHODS FOR STRUCTURAL ANALYSIS DURING CONSTRUCTION PHASE

Claudius Schmitt¹, Hans Neuner², Benjamin Kromoser³

¹TU Wien, Department for Geodesy and Geoinformation – Engineering Geodesy, (Claudius.Schmitt@geo.tuwien.ac.at)

²TU Wien, Department for Geodesy and Geoinformation – Engineering Geodesy, (Hans.Neuner@tuwien.ac.at)

³BOKU, Institute of Structural Engineering (IKI), (benjamin.kromoser@boku.ac.at)

Key words: *Modelling point cloud; freeform approximation; structural analysis; finite element model; shell structure*

ABSTRACT

I. INTRODUCTION

Surface based inspection measurements are one of the main issues in engineering geodesy. During a new construction process of a pneumatic formed hardened concrete shell, surface based measurements and analysing procedures are realised. The concrete shell is built as a dome and further prepared as a deer pass bridge over a two-track rail. As learning structure a 1:2 model was built where the construction process, the measurement and analyse concept could be tested. The result of surface based measurements are scanned 3D point clouds performed inside of the dome. They provide the possibility of modelling a freeform surface for structural analysis and the analysis of the deviations between the actual cloud and the CAD model. The analysis concept includes the geometric surface approximation as well as the surface and the point based deformation analysis of the actual geometry during different construction steps.

Designing the construction was part of the Institute for Structural Engineering, while the surface based geometric monitoring is realised by the Research Group Engineering Geodesy, both at the TU Wien. The project is advertised and managed by the ÖBB-Infrastruktur AG.

This paper focuses on the requirements of the structural analysis for the measurements and their approximation process.

In the modelling part, the point cloud is approximated by estimating the control points of a B-Spline surface in a least squares adjustment.

First the project is described. In the second chapter the engineering geodesy part is accomplished with the measurement concept, the coordinate system definition and the B-Spline surface approximation. The third chapter complete the paper with the analysis process during the construction phase under considerations of the requirements of the Finite Element Model (FEM). The paper will close with the conclusion and future tasks.

A. Project and Motivation

Building a new rail line between Graz and Klagenfurt, the Koralm rail way, is one main infrastructure project of the ÖBB-Infrastruktur AG (federal railway in Austria), managed by the PLK2 team and the technical department SAE / Bautechnik-Brückenbau, (ÖBB-Infrastruktur). In the section Aich – Mittlern, three deer passes are planned over the two-track rail, described in more detail in (Kromoser et al. 2018b, a). One of these passes is built as a shell bridge with the method of pneumatic forming of hardened concrete. A flat hardened concrete plate is transformed into a double curved concrete shell, by inflating a simple air cushion, placed under the concrete plate, and stressing post-tensioning tendons at the circumference, see Figure 1. The geometry of the lifted shell is a main-axis symmetric freeform surface with a membrane-stress-state characteristic. This means negligible transversal shearing and bending stress. This dome is mostly used as formwork for the end layer of shotcrete.



Figure 1: Wildbrücke after the lifting process with iron beams minimizing the shear stress

The manufacturing process of this light weight structure was developed at the Institute for Structural Engineering, further described in (Kromoser B. et al 2014, 2015a, b) and transformed to the industrial realization with the ÖBB-Infrastruktur AG. The dimension of the deer pass is ~53m by ~38m and ~8m high. As learning structure for the construction process a 1:2 scaled learning structure was previously build. The only difference to the deer pass are the cutting

areas. According to the subsequent utilization, parts of the domes are cut out, in case of the deer pass the ends with higher curvature, to get a bridge and in case of the learning structure getting a pavilion, see Figure 2.

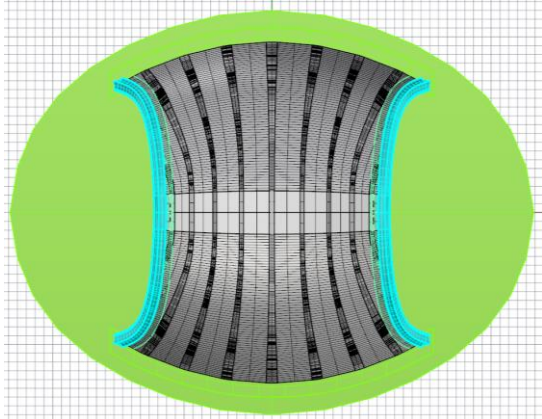


Figure 2: Wildbrücke - Top view to the final bridge in grey with cutting edges in turquoise green and the bottom plate in green

Because of the high sensitivity of the shell against geometric imperfections, the geometry needs to be planar monitored after each stress relevant construction step, determining the actual geometry and the surface based deviations to recalculation and evaluate the static load behaviour of the actual geometry. In case of the deer pass after the lifting process, the additional concrete slices on top, the soil filling process for the ramps and during removing the tension plate as last critical step. The engineering geodetic tasks at each construction step were first the inspection of the geometry and second the approximation of the actual freeform geometry for the structural analysis. (Kromoser 2015)

II. MEASUREMENT AND ANALYSIS

A. Measurement Concept

The measurement concept was separated into three types. First the net measurements to define the fix points inside of the shell mounted to the bottom plane. Second the monitoring with surface based and point based measurements insight the air cushion. At last, the point based monitoring during the removal of the tension plate. The measurement configuration is shown in Figure 3 with the stations in the centre, the four fixed points at the tension plate and the 48 prisms in four vertical layers mounted directly on the shell. Three types of prisms were applied according to the required repeatability accuracy for the centring (ordered by their accuracy level, from lowest to highest): Leica round prisms for the demolition parts of the shell, Leica mini prisms for the upper shell and sphere prisms with industrial adapters for the lowest layer.

The reason for the scanning total station's position in the centre at 2 m height was the incidence angle of the laser beam with the dark air cushion. The other stations were positioned nearby because of the same usage of the fixed points and in order to prevent being in the line

of sight of the laser beam from the scanning total station. The bottom fixed points on the plate were determined by net measurements to the four survey pillars around the construction side. To obtain full 3D coordinates with homogeneous accuracy, the height was implemented by precision levelling of the bottom fixed points instead of tape measurements to the tilting axis of the instruments. In case of the levelling and for accuracy reasons sphere reflectors for the fixed points were also used.

In case of the deer path the values for the accuracy were derived from the load behaviour of the shell to 1cm for the maximum displacements at the bottom edge and to 10 cm for the maximum displacement for the rest of the shell. These values need to be interpreted as tolerances, thus resulting in a standard deviation of ~2mm and ~2cm respectively for the measured geometry. However, relative tendencies of displacements should be detected with less than 1mm and 1cm respectively.

The discretisation level of the object was set to 3cm. The reason for defining these thresholds are presented in chapter III.A.

B. Coordinate Systems

Five coordinate systems are named in this project, whereby primarily the transformation parameters between them are defined. These coordinate systems can be divided into two groups: the planned and the object oriented. The transformation parameters inside the planned group are defined at the beginning of the construction process and the ones inside the object oriented group depend on the actual object, the shell and the bottom plane. All of them are metrical 3D Cartesian coordinate systems except the global one, which is a separate 2D+1D Gauss-Krüger projection system.

Below a short overview of the systems with their scaling, transformation parameters and left or right hand (rh/lh) definition is given. The used nomenclature for the transformation parameters with is introduced subsequently in the text.

Planning Systems:

- Local / FEM: [mm], rh
- Construction: [m], lh, $\{rZ_{Pl}, tX_{Pl}, tY_{Pl}, tZ_{Pl}\}$
- Global: [m], lh, $\{rZ_{Pl}, tX_{Pl}, tY_{Pl}, tZ_{Pl}\}$, including geometric reductions and mapping distortions.

Object oriented systems:

- Object local: [mm], rh, $\{rX_{bp}, rY_{bp}, rZ_{shell}, tX_{shell}, tY_{shell}, tZ_{bp}\}$
- Object best: [mm], rh, $\{rX_{shell,all}, rY_{shell,all}, rZ_{shell,all}, tX_{shell,all}, tY_{shell,all}, tZ_{shell,all}\}$
- Object level / FEM: [mm], rh, $\{rZ_{shell}, tX_{shell}, tY_{shell}, tZ_{bp}\}$

Figure 3 shows an example of the planned coordinate systems with the shell before and after the inflation process. Around the shell are the survey pillars transferring the system to the construction side.

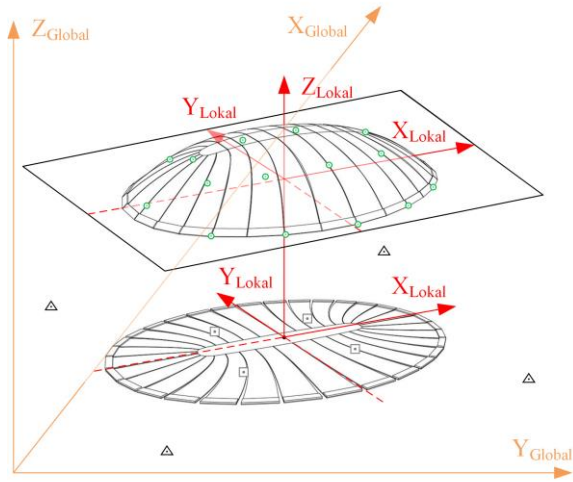


Figure 3: Planning coordinate systems, Global (brown) and Local (red), with survey pillars (black triangles), bottom plane points (grey square), monitoring prisms (green circles)

Planning System

The *Local / FEM* coordinate system is the right hand geometry design system of the shell. The origin is defined as the intersection of the two main axes of the shell at the bottom edge. The X and Y axes are defined along the shell's main axes respectively. The Z axis is rectangular to the (X, Y) plane and oriented to the gravity direction. The structural analysis and the geometry optimization were performed in the planning state in this system.

The *Construction* coordinate system is a left hand system and derived from the *Global* coordinate system as combination of 1D and 2D to a full 3D-system without any geometric reductions or projection distortions. The transformation between the *Construction* and the *Local* system is defined the translation tX_{Pl} , tY_{Pl} , tZ_{Pl} and the rotation around the Z-axis, rZ_{Pl} . Thus, it maintains the vertical alignment as in the CAD planning system. It's used for the 2D staking out process and the deviation values after the lifting process between the actual and the nominal state including the rigid-body movement.

The *Global* coordinate system is the left hand 2D ÖBB Gauss-Krüger projection coordinate system with a separate 1D-height system. The survey pillars around the construction site are positioned in both systems, the *Global* and *Construction* one. This system serves as reference system of the ÖBB. Different to the *Construction* coordinate system this one includes geometric reductions and projection distortions.

All Object oriented systems are right hand systems.

The *Object local* coordinate system is locally defined on the actual object. The ground plane (gp) represents the bottom edge of the shell. It contains the origin and is perpendicular to the Z-direction. The X&Y-directions are defined by the actual geometry of the shell. Therefore, a horizontal slice of 0.7 m beginning by 1m from the ground plane was taken to run an iterative closes point algorithm, ICP, between the point clouds representing the actual and the nominal geometries. The estimated parameters indicate the

translations in X and Y direction and the orientation of the X-axis with respect to the *Local* coordinate systems. Starting with the *Construction* coordinate system and its given transformation with parameters rZ_{Pl} , tX_{Pl} , tY_{Pl} , tZ_{Pl} to the *Local* system and transforming these system with the transformation parameters mentioned above $(rX_{bp}$, rY_{bp} , rZ_{shell} , tX_{shell} , tY_{shell} , $tZ_{bp})$ to the *Object Local* system the parameters describe the rigid-body movement of the object (bottom plate + shell) during the construction and lifting process. After these transformation the deviations between the nominal and actual object's geometry, represents the relative object deviations-

The *Object best* coordinate system is completely oriented on the actual geometry of the shell. Distinct to the *Object local* coordinate system its spatial orientation results from a best-fit transformation of the entire point clouds between the shell's actual and nominal geometry. The starting configuration is the actual cloud in the *Object local* coordinate, which is matched by an ICP to the *Object best* coordinate system. It shows the best match of the actual shell geometry, with smallest deviation to the nominal geometry overall.

The *Object level / FEM* coordinate system is an inverse transformed *Object local* system to a level aligned system taking the inverse transformation parameters rX_{bp}^{-1} rY_{bp}^{-1} after the determination of the parameters of the *Object local* system. It is used to represent the geometry in an object related levelled coordinate system for the structural analysis.

C. Surface Approximation

As mentioned in section A the scanned point cloud with an object resolution of 3 cm was approximated with a B-Spline surface. The following figure describes roughly the procedure of the point cloud approximation process.

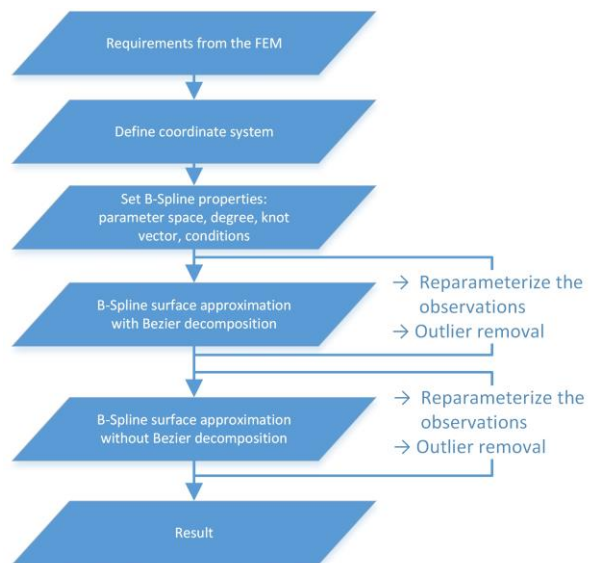


Figure 4: B-Spline surface approximation process

Further on, the approximation model and the boundary conditions are described in more detail. The remaining steps including the reparameterization of the observations, the behavior of the function in case of outliers and setting the B-Spline function parameters are beyond the scope of this paper.

The approximation model is a least squares adjustment, described in (Schmitt et al. 2014; Bureick et al. 2016) using the parametric definition of the B-Spline surface function (Piegl and Tiller 1997).

$$C(u_c, v_c) = \sum_{i=1}^{n+1} \sum_{j=1}^{m+1} N_{i,p_u}(u_c) N_{j,p_v}(v_c) CP_{i,j} \quad (1)$$

u_c, v_c are the parametric values of the surface point C coordinates X, Y, Z. The parameter space and the parameters of the observations are defined in a first step at the edge of the point cloud and calculated iteratively before the adjustment. N_{i,p_u}, N_{j,p_v} are the basis functions in u and v direction of the parametric space, defined according to the surface point position u_c, v_c . p_u, p_v provide the related degree of the $n + 1$ and $m + 1$ basis functions respectively. $CP_{i,j}$ are the control points and the unknowns in the least squares adjustment. With their coordinate values X, Y, Z, they represent the link between the parametric space and the Cartesian space. The used approach differs from (Ezhov et al. 2018) or (Paffenholz et al. 2018), by using the parametric definition and directly the inhomogeneous spaced 3D-points as observations. The knot vectors are defined in a closed form in U and V direction over the space from 0 to 1 with $p_u + 1$ and $p_v + 1$ multiple knots at the beginning and at the end.

$$U = \left(\underbrace{0,0,0,0}_{p_u+1}, k_{internal,u}, \underbrace{1,1,1,1}_{p_u+1} \right); \quad (2)$$

$$k_{internal,u} = 0.128, 0.244, 0.350, 0.451, 0.550, 0.651, 0.756, 0.872;$$

$$V = U;$$

$$\xrightarrow{\text{yields}} N_{1,p_u}(0) = N_{n+1,p_u}(1) = N_{1,p_v}(0) = N_{m+1,p_v}(1) = 1$$

Beside the classic requirements to approximate a mean surface from noisy observations the requirements to the geometry for the structural analysis need to be taken into account. The most important requirements from the latter category are to provide a clear bottom edge, representing the support of the shell and to find an interpretable description in case of the analytical definition of the geometry for the FEM software. Further requirements from this 2nd category can be summarized as follows:

1. General structure dependent and process requirements
2. Interface requirements

3. Time interval requirements
4. FE calculation requirements

The topics are described in more detail in chapter III.

The implementation of the requirements especially the bottom edge definition was done by the extension of the Gauss-Markov-model with restrictions. The restrictions are different to the parametrization of the observations with the coons patch and the stochastically tightening of the surface to the boundary curve described in (Harmening, C. and Neuner 2015).

Due to the requirement of representing a clear support of the shell a stronger restriction in the Z-component is needed. Therefore, the domain definition of the B-spline surface function is changed, by restricting the Z-component of the bottom edge control points, \widehat{CP}_Z , to zero.

$$\begin{aligned} B_{1...12}: \widehat{CP}_Z_{i,j} &= 0; \quad i = 1; \quad j = 1 \dots 12; \quad (3) \\ B_{13...24}: \widehat{CP}_Z_{i,j} &= 0; \quad i = 12; \quad j = 1 \dots 12; \\ B_{25...36}: \widehat{CP}_Z_{i,j} &= 0; \quad i = 1 \dots 12; \quad j = 1; \\ B_{38...48}: \widehat{CP}_Z_{i,j} &= 0; \quad i = 1 \dots 12; \quad j = 12; \end{aligned}$$

The least squares adjustment with the mentioned restrictions is solved according to (Niemeier 2008).

This type of conditions can be applied only if the geometry is in the appropriate *Object level / FEM* coordinate system with the bottom plate height set to zero and oriented to gravity. Beside the restrictions $B_{1...48}$ in the Cartesian coordinate system, “edges” in the B-spline surface domain needs to be defined equivalently. Hence two assumptions are necessary.

First, the control points needs to be aligned on the bottom edge. This depends on the parameter space definition, i.e. where start and end edges of the parameter space correspond to the bottom edge in the Cartesian space. This edge is divided into four sections equivalent to B-Spline curves. They represent the maximum respectively minimum values in u and v direction of the parameter space of the B-Spline surface. Three of these edge curves are shown together with the associated control points in the following figure.

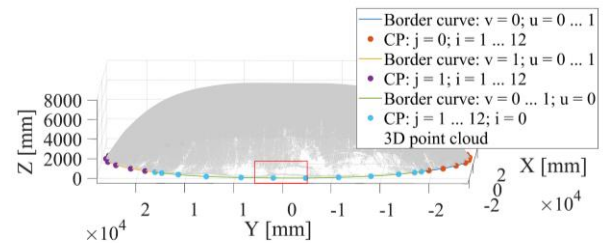


Figure 5: Point cloud with bottom edge and control points in the restricted case

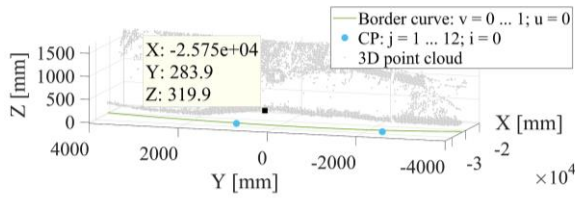


Figure 6: Bottom edge section with difference in the point cloud edge and the required bottom edge

The second assumption is to get this clear edge definition in the function space; means to assign the knot vector definition from the beginning and the end $(\{0,0,0,0, \dots, 1,1,1,1\})$ to each knot position, which implicit defines the edge position. Consequently, the location of the control points is on top of the B-Spline surface; this means they are part of the surface along the bottom edge. Four control points with the related basis functions contains already this property due to the closed form of the knot vector at the beginning and end, see eq. (1). For the remaining 44 control points and basis functions, 10 on each edge, the knot vector in u and v direction requires a modification. The modification is the extension of the knot vector U by multiplying the internal knots p_u times, e.g.

$$k_{internal,u} = \underbrace{0.128, 0.128, 0.128}_{p_u}, \underbrace{0.244, 0.244, 0.244, \dots}_{p_u};$$

and p_v times in v direction respectively. This decomposes the entire B-spline surface into $C0$ -connected Bezier patches between different knot values. The problems arising from this definition in the approximation are the decreased continuity at the edges between the patches. In the approximation the decreased continuity appears depending on the local unevenness of the surface, which can be seen in the following figure.

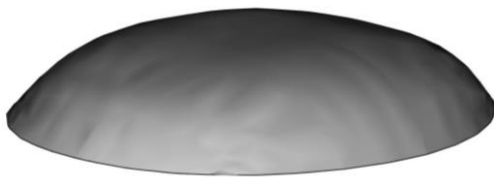


Figure 7: B-Spline surface with $C0$ reduced Bezier patches edges

This geometry is not suitable for FEM as in our case the second derivative is analytical needed for the FEM analysis of this object structure. Further explanations are given in detail in the next chapter.

As a next step the parameters of the observations are optimized in consequence of the enlargement of the parameter space. This difference can be seen in Figure 6, where the marker on the point cloud represents the edge of the point, which is ~ 32 cm above the restricted new bottom edge curve and the initial edge of the parameter definition in B-spline function space. If this

is done the last step will perform the approximation, calculated with a knot vectors without multiple internal knots and the new parameters of the observations, but still with the restrictions to the CP's. Although they aren't directly located to the surface but closed by, except the four CP's at the beginning and end. This results in a smoother more generalized surface with $C2$ continuity, shown below.



Figure 8: 12x12 B-Spline surface used as geometry for the FEM

The restriction is still necessary in our case because the point cloud is missing in some areas as mentioned before. Nevertheless, with the restricted CP's in combination with the adapted parameter space and the knot vectors with single internal knots, the bottom edge of the geometric model shows displacements smaller than 5mm, satisfying the bottom edge and the other FEM requirements to the surface.

For this B-Spline surface the residuals of the approximation are shown below. The residuals consists of the errors from the sensor, the B-Spline model and the actual geometry assuming, that the measured surface do not represent the required geometry for the structural analysis. The structural engineers assessed the geometric result obtained by this approximation approach as representative for the structural analysis.

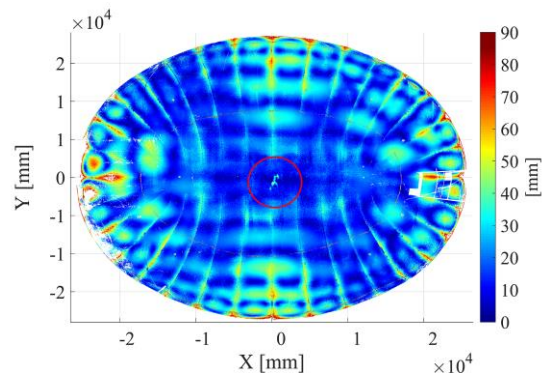


Figure 9: Residuals of the B-Spline approximation with 12x12 control points, single internal knot vectors and bottom edge restriction and signaled Air cushion folds

A purely geometric approximation optimized with respect to the sensor's accuracy, can be seen below.

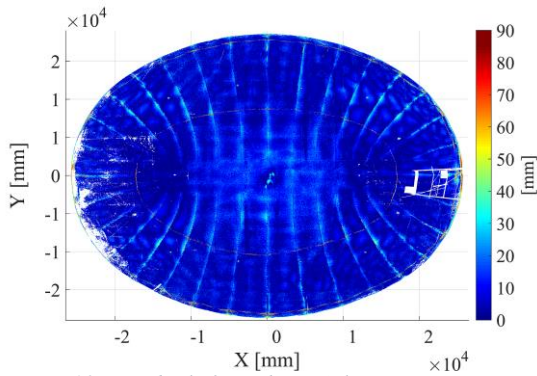


Figure 10: Residuals from the B-Spline approximation with 30x30 control points, single internal knot vectors and bottom edge restriction.



Figure 11: Approximated B-Spline surface with 30x30 CP

The approximation is similar to the one before but contains more unknown parameters in terms of CP's. The number of CP's is increased to 30x30. The residuals are much smaller than the residuals of the 12x12 approximation and distributed more homogeneous over the shell's surface. Still, some systematic effects in the form of bubbles, which can be observed in the neighborhood of the edges. This effects will be analyzed in future work for a deeper understanding of the B-Spline surface function.

The 30x30 surface cannot be used in the FEM, due to restrictions in the maximum number of manageable control points and in case of an generalized smooth surface.

III. FREEFORM GEOMETRY 4 FEM

A. General

This chapter introduces the requirements of the FEM for a suitable actual geometric model. Some of these requirements are general, some are very specific to the software and the structure.

This shell structure is specially designed as a shell with membrane properties. The membrane model form a chain line where primarily normal forces occur. The material is presumed isotropic with a linear elastic behaviour. In the used RFEM software the shell is modelled with Midlin elements and calculated by the Timoshenko solution approach for shell structures. (Dlubal Software 2018).

The interface between the approximated geometry and the FEM is the mesh and its generation on this geometry.

In a shell model the geometry represents the 2D chain line surface or the intermediate surface. This surface

lies between the inside and outside surface of the structure and cannot be measured directly. The requirements of the FEM help to produce a best possible intermediate surface.

One main issue is not losing geometric accuracy or information in the connections between the different processing steps and the adaptation of the geometric and the requirements of the FEM.

Figure 12 shows an FEM geometry optimization workflow when using actual geometry. It starts with the planned CAD geometry and uses subsequently the actual geometry in an optimization loop. Beside the steps itself the connection between them, the time schedule and optimisation rate of the process as well as the requirements to the geometry from the Finite Element Analysis (FEA) are described in more detail later on.

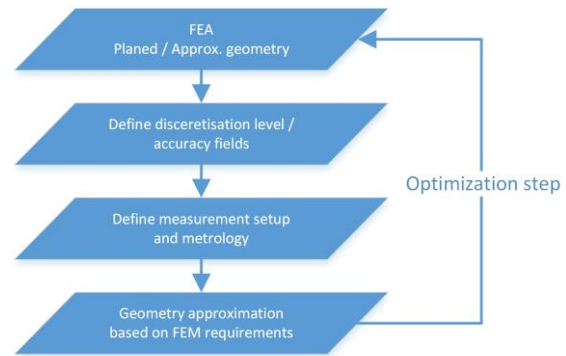


Figure 12: FEM - Geometry update sequence

In a first step the structural behaviour is analysed by simulating different load behaviours for the structure based on the reference geometry. This reference geometry can already be the actual surface or a planned surface.

In the second step the required accuracy of the approximated geometry including the measurement and approximation accuracy can be derived from the virtual displacements and the deformation simulations under different loads in the FEA. Using this approximation accuracy as well as the size of the reaction area of different load behaviours and, the consequences of the buckling effect the object's discretization level can be estimated. The accuracy and discretisation level can change over the structure und need to be accounted in the measurement plan.

Out of these results the requirements to the measurement plan, including measurement setup and choice of the metrology are derived in the third step. These determinations of discretisation and accuracy levels result from interpreting the FEM outcomes and need therefore to be interpreted as tolerance values. Their conversion to standard deviations follows the approach given in (Heuncke et al. 2013).

The fourth step consists of the approximation of the measured data under consideration of the derived accuracy and discretisation levels. A main geometric property, which needs to be considered is the reduction from the measured surface to the intermediate surface. This corresponds to a generalisation step under boundary conditions, e.g. the supports seen in Figure 13.

The optimization steps depend on different factors. One of these is the displacement between the nominal and the actual geometry. If this value is outside the expected range, the structure needs to be recalculated, because of a changed load behaviour. If the load behaviour changes the accuracy and discretisation level could change. Hence the further steps needs to be adjusted as well.

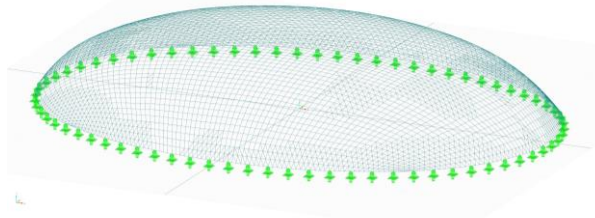


Figure 13: FE mesh with supports

B. Requirements of the FEA

Based on the approximated geometry the FE-mesh, consisting of the FE-knots and the topology between them, needs to be generated. The design and optimization (mesh refinement) of the mesh consists of the design of the FEM calculation, the structure, the material model and the load conditions, e.g. (Zienkiewicz et al. 2013) and at the end of the mesh process the evaluation with the knowledge from the structural engineer.

Basic criteria of the mesh generator in RFEM defining the form of the FE-elements are the maximum edge length, the distortion of the mesh elements w.r.t. the unitary elements and the maximum slope between the elements and the geometry. The values of these parameters were chosen in our project by default and changed after validating the results by the structural engineer, e.g. high stress in irregular areas are not realistic. Because of this less tangible evaluation of the results, we focus subsequently on the continuous surface description, the boundary condition and the coordinate system.

The continuous description is necessary for the optimal definition of the FE mesh. In this project the surface representing the structural behaviour is continuous (no discontinuities and joints). At a first look, it seems easier to divide the surface into well approximated patches. However, in this case one faces the challenge of compensating the junctions at the patch edge and interpreting the accuracy at this positions. A further challenge is to distinguish edges, which are structural relevant as they may represent different construction sections, boundary conditions or material changes. FEM knots need to be placed on this kind of edges, while the other edges have to be ignored and the surface interpreted as continuous. If the geometry fulfills this properties it conforms to a waterproof required geometry.

The representing geometry of the structural behaviour is in this project the so-called intermediate

surface of the membrane stress state. As already mentioned this intermediate surface cannot be measured directly. In case of the deer-path this surface is derived from the measured inside surface. The shift of the inside surface to the intermediate surface is negligible because of the symmetric design and the constant thickness. More important on the assumption of the consistent thickness and continuous progression is to smooth or generalise the measured Surface. Means to reduce the superficial irritations mostly caused by the folds of the air cushion. The folds of the air cushion emerge, when the shell is concrete in the flat state on top of the flat uninflated cushion lying on the bottom plate. The influence of this folds are up to 5cm and can be seen in the residuals at the approximation in the centre of the shell in Figure 9.

The surface edges are particularly important as they define the supports where the load is concentrated. In this parts the requirements to the geometry differs to the rest of the surface, especially in terms of the geometric accuracy. Both conditions mentioned above are part of the so-called boundary conditions of the FEM.

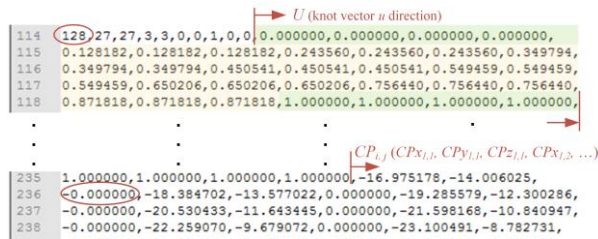
To fulfill this requirements the surface needs to be extrapolated from the measured 3D point cloud, seen in Figure 6. Thus, completeness of the object's geometry is as important as the boundary condition.

The importance for this geometry part can also be seen on the support displacements tolerances, which are 10 times smaller than on every other geometry position of the shell. This depends on the special design of supporting a shell structure with a membrane stress state.

The coordinate system used in the software is 3D Cartesian. For this structure the load is the dead weight of the shell and the weight of the ground forming the ramps. The value and direction of these loads is oriented to gravity. The easiest way to account for this fact is orienting an axis also to gravity. This is done by default with the Z Axis. The measured surface should also be represented in this coordinate system. The realisation of the measured frame is already described in chapter II.B.

C. Interface

The interface between the software products, means mostly the data exchange between them. First, the possibility of supported standardized data formats or direct links needs to be found out and second the definition of the geometry inside this data formats or direct links needs to be specified. In our case the supported data formats were the Initial Graphics Exchange Specification (IGES) and Standard Triangulation/Tesselation Language (STL). Our decision felt to IGES because in these format definition the analytical parameters of the B-Spline surface were documented instead to the STL format, where interpolated triangles calculated on the B-Spline surface, were stored. A short description can be seen in the following figure.



114	128	27, 27, 3, 3, 0, 0, 1, 0, 0, 0, 0.000000, 0.000000, 0.000000, 0.000000,
115	0.128182, 0.128182, 0.128182, 0.243560, 0.243560, 0.243560, 0.349794,	
116	0.349794, 0.349794, 0.450541, 0.450541, 0.450541, 0.549459, 0.549459,	
117	0.549459, 0.650206, 0.650206, 0.650206, 0.756440, 0.756440, 0.756440,	
118	0.871818, 0.871818, 0.871818, 1.000000, 1.000000, 1.000000, 1.000000,	
235	1.000000, 1.000000, 1.000000, 1.000000, -16.975178, -14.006025,	
236	0.000000, -18.384702, -13.577022, 0.000000, -19.285579, -12.300286,	
237	-0.000000, -20.530433, -11.643445, 0.000000, -21.598168, -10.840947,	
238	-0.000000, -22.259070, -9.679072, 0.000000, -23.100491, -8.782731,	

Figure 14: Excerpt of an IGES file with B-Spline definition

The iges file is roughly divided in four parts (Header, summary of the defined geometry models, geometry model definition, end). Each geometric model has its own key. 128 stands for B-Spline surfaces as parameter definition, followed by the values of the knot vectors in u and v direction and the control points (X, Y, Z). The approximation condition of the surface edge connecting the bottom plane can be seen on the zero values of the Z-coordinates of the control points, seen in Figure 14.

Other Software products have the opportunity to receive data directly by a CAD software link. In that case the file interpreter on the import and export side are omitted, which contains fewer errors because of misinterpretation or missing format specification. A type of misinterpretation was for example, that it's not possible to import the surface without separate edge lines to receive the correct unit definition for the surface. In our case the FEM software Drubal RFEM Version 5.12 was used.

The next software restriction was the maximum supported number of 100 control points followed by a continuously surface description with boundary conditions. This means, that a surface construction of patches or trimmed surfaces could not be reliably interpreted.

The misinterpretation of the edges of the trimmed surface results from their definition. The trimmed B-Spline curve is an interpolated curve on the B-Spline surface and cannot be derived analytically from the surface definition, when it runs beside the parameter line, as was here the case.

When the interpolation of the B-Spline curve (trim curve) onto the B-Spline surface is not close enough, the software does not interpret the curve as trimming curve of the surface and take the original surface as edge definition to fulfill the waterproof condition.

The work around to get a clear edge definition is to consider it by the approximation as condition as mentioned above. This is a general problem by using laser scanners, because the edges of the point clouds are never clear defined and needs further information to be modelled in the approximation step.

D. Time interval

The time interval is controlled by the economics and by the construction process itself.

The economic aspects are the classic ones, doing less measurements and when doing measurements keeping the downtime of the construction process as short as possible.

The downtime or reaction time by unexpected behaviour of the construction, is the matter of negotiation of all stakeholders. The reaction time was set to one day with a period of one day where the measurements, analysis and result visualisations needs to be done. The construction relevant steps were the geometry can change due to changes in the structure and its load behaviour, changes in the material composition or changes of the external loads onto the structure during the construction phases. In this project the first impact to the construction is the stiffening of the inflated shell by the grout topping layer combined with additional reinforcement. This step is essential because afterwards the deviations of the geometry have higher impact on the load behaviour than before.

The change of the external load occurred by unsymmetrical ground filling of the ramps on both sides of the bridge. Simulations shows high impact to the geometry at this steps, so that the point based monitoring was performed all 30 Minutes and at night the surface based scanning was realised. Beside that smaller monitoring units were realised, to learn the behaviour of the new structure on different influences.

IV. CONCLUSION AND OUTLINE

As shown in this project the determination of the geometry of new structures is getting more and more important. Therefore, a concept was developed, which includes the shape verification and the analysis of the static behavior from the beginning of the construction process. Therefore, a process have been developed producing a suitable geometry for the structural analysis. The process includes the information of the pre-analysis of the structural behavior and take them into account during the measurement and approximation process. Emphases of the geometric approximation are the boundary condition, the geometric completeness, the measurement and processing duration and the interfaces between B-Spline surface and the FEM program. The prioritization of the FEM requirements and the optimization of the approximation process in case of generalized surfaces as well as the outlier detection are elements of current and future research.

V. ACKNOWLEDGEMENTS

Many thanks to the ÖBB INFRA to build this Prototype in real dimensions at the Koralmbahn railway. Thanks also for the good cooperation and constructive discussions with the Institute for Structural Engineering to give us the chance to apply our ongoing research on surfaced based B-Spline approximation for structural analysis.

References

- Bureick J, Neuner H, Harmening C, Neumann I (2016) Curve and Surface Approximation of 3D Point Clouds. AVN 123:315–327
- Dlupal Software (2018) Handbuch RFEM 5 - Räumliche Tragwerke nach der Finite-Elemente Methode

- Ezhov N, Neitzel F, Petrovic S (2018) Spline approximation, Part 1: Basic methodology. *J Appl Geod* 12:139–155. doi: 10.1515/jag-2017-0029
- Harmening, C. C, Neuner H (2015) Continuous modelling of point clouds by means of freeform surfaces. *Österr Z Für Vermess Geoinformation VGI* 103. Jahrgang; Austrian Contributions to the XXVI General Assembly of the International Union of Geodesy and Geophysics (IUGG):188–197
- Heunecke O, Kuhlmann H, Welsch W, et al (2013) *Handbuch Ingenieurgeodäsie: Auswertung geodätischer Überwachungsmessungen, 2., neu bearbeitete und erweiterte Auflage*. Wichmann Verlag
- Kromoser B (2015) *Pneumatisches Verformen von ausgehärtetem Beton*. TU Wien
- Kromoser B, Kollegger J, Kari H, et al (2018a) Practical Application of an innovative concrete shell construction method: Construction of the deer pass AM2 by use of PFHC. *Beton- Stahlbetonbau* 113:222–232
- Kromoser B, Pachner T, Tang C, et al (2018b) Form Finding of Shell Bridges Using the Pneumatic Forming of Hardened Concrete Construction Principle. In: *Adv. Civ. Eng.* <https://www.hindawi.com/journals/ace/2018/6309460/>. Accessed 30 Nov 2018
- Niemeier W (2008) *Ausgleichsrechnung: Statistische Auswertemethoden, 2., überarb. und erw. Aufl.* de Gruyter, Berlin
- Paffenholz J-A, Hüge J, Stenz U (2018) Integration von Lasertracking und Laserscanning zur optimalen Bestimmung von lastinduzierten Gewölbeverformungen | Integration of Laser Tracking and Laser Scanning for Optimal Detection of Load Induced Arch Displacement. *Allg Vermess-Nachrichten Avn* 125:
- Piegl LA, Tiller W (1997) *The Nurbs Book*. Springer
- Schmitt C, Neuner H, Neumann I, et al (2014) Erstellung von Ist-Geometrien für strukturmechanische Berechnungen. In: Wieser A (ed) *Beiträge zum 17. Internationalen Ingenieurvermessungskurs Zürich*. Wichmann Verlag, Heidelberg, pp 37–48
- Zienkiewicz OC, Taylor RL, Zhu JZ (2013) *The finite element method. [Vol. 1]: Its basis and fundamentals, 7. ed.* Elsevier, Butterworth-Heinemann, Amsterdam